17

Reversal-tolerant Catalyst Layers

Siyu Ye

17.1 Introduction

Fuel cells present a promising technology for providing clean, efficient electric power in a variety of applications. They are the most environmentally friendly alternative to internal combustion engine technology in vehicles. They also have applications in portable electronics, as well as distributed and back-up power. The last few years have witnessed a tremendous increase in the research and development of fuel cells, including the development of new materials, new system designs, and new operating methods. While many breakthroughs have been made, technical and economic barriers for commercialization still exist. For a polymer electrolyte membrane fuel cell (PEMFC) – the most promising fuel cell technology – to be used commercially in stationary or transportation applications, cost and durability are the major challenges. In transportation applications, fuel cell technologies face more stringent cost and durability requirements: a fuel cell system needs to cost less than $50/kW with a 5,000 hour lifespan (150,000 miles equivalent) and have the ability to function over the full range of vehicle operating conditions (–40 to +90 °C). For stationary applications, a fuel cell system operating on natural gas needs to achieve 40% electrical efficiency and 40,000 hours durability at $750/kW [1]. To be commercially viable, however, fuel cell systems must also exhibit adequate reliability in operation, even when the fuel cells are subjected to conditions outside the preferred operating range. As PEMFCs approach commercialization, significant progress is being made towards producing systems that achieve the optimum balance of cost, efficiency, reliability, and durability.

The ability of the fuel cell to operate under a wide range of conditions with different system characteristics is described by the term “fuel cell operational flexibility”. Optimum fuel cell operational flexibility must take into account both specified conditions and an estimated amount of unexpected, or “out-of-specification”, conditions over the fuel cell target lifetime. Some of the conditions to consider include: reactant composition and flow rates, operating and environmental temperature and pressure, humidification levels, peak load

requirements and turn-down ratios, duty-cycle characteristics (including percentage of time at different load points), and required rate of transient responses.

Some factors are known to affect the life of PEM fuel cells. While platinum is an exceptionally active catalyst, its performance can quickly degrade. For PEMFC durability, deterioration in fuel cell performance is mostly due to degradation of the electrocatalyst, in addition to membrane degradation [2]. A number of mechanisms can contribute to catalyst degradation, including: catalyst agglomeration and catalyst dissolution/migration [3, 4]. It was found that Pt particle size increase is accelerated by potential cycling [3, 4]. It has also been observed that the size and morphologies of the Pt nanoparticles varied greatly from the cathode surface to the cathode-membrane interface after potential cycling [5, 6]. Carbon oxidation and corrosion has been observed during PEM fuel cell start-up and shutdown operations [5, 7–9]. Mass transport properties degrade as a result of the accumulation of excess water in the gas diffusion pores [10, 11]. Impurity ions affect the membrane proton conductivity and oxygen reduction kinetics [12, 13]. In addition to membrane degradation, catalyst oxidation/dissolution, catalyst sintering, and cathode carbon corrosion, anode voltage reversal also severely affects fuel cell durability and reliability [14–18]. The development of a reversal-tolerant catalyst layer will be reviewed here.

During normal operation of a PEM fuel cell, fuel is electrochemically oxidized at the anode catalyst, typically resulting in the generation of protons, electrons, and possibly other species, depending on the fuel employed. The protons are conducted from the reaction sites at which they are generated, through the electrolyte, to electrochemically react with the oxidant at the cathode catalyst. The electrons travel through an external circuit, providing useable power, and then react with the protons and oxidant at the cathode catalyst to generate water as the reaction product.

In operation, the output voltage of an individual fuel cell under load is generally below one volt. Therefore, in order to provide greater output voltage, multiple cells are usually stacked together and connected in series to create a higher voltage fuel cell stack. End plate assemblies are placed at each end of the stack to hold the stack together and to compress the stack components together, thereby sealing and providing adequate electrical contact between various stack components. Fuel cell stacks can be further connected in series and/or parallel combinations to form larger arrays for delivering higher voltages and/or currents. However, fuel cells in series are potentially subject to voltage reversal, a situation in which a cell is forced to the opposite polarity by the other cells in the series. This can occur when a cell is unable to produce the current forced through it by the rest of the cells. It is possible that one or more membrane-electrode assemblies (MEAs) or groups of cells within a stack, or even a complete stack in a multi-stack system, can be driven into voltage reversal by other stacks in an array. Several conditions can lead to voltage reversal in a PEM fuel cell, including insufficient oxidant, fuel, or water, low or high cell temperatures, and certain problems with cell components or construction. High reactant utilization is generally required for most applications in order to maximize fuel efficiency and reduce system parasitic load, size, and weight that may be associated with the oxidant and fuel delivery and/or storage systems. Transient operation, particularly under the demanding

conditions of automotive applications, introduces greater challenges due to rapid load changes and the resulting wide range of conditions.

During high overall stack utilization, uneven flow sharing between cells can result in partial fuel and/or air starvation conditions in individual cells. A lack of system response during a sudden change in reactant demand will lead to fuel and oxidant starvation. This situation can be exacerbated by the presence of liquid water in channels or by other blockages, resulting in further flow sharing difficulties that in extreme cases can lead to complete starvation conditions. One example of such a condition is sub-zero start-up or operation. As long as the stack temperature remains below zero Celsius, the cells are prone to ice formation and subsequent flow channel blockage. Figure 17.1 [15] presents the change in cell voltage and the equivalent module power with time during freeze start-up from –15 °C. Negative values in the cell voltage for some cells can be clearly observed in the early stage of the freeze start-up. Although stack and system operation can be designed to reduce these occurrences, it is generally accepted that rapid heating of the stack to minimize ice formation is desirable. Alternatively, a flow field channel may be blocked due to deformation or inert gas blanketing the MEA. Reversal generally occurs when one or more cells experience a more extreme level of one of these conditions compared to other cells in the stack. While each of these conditions can result in negative fuel cell voltages, the mechanisms and consequences of such a reversal may differ, depending on which condition caused the reversal.

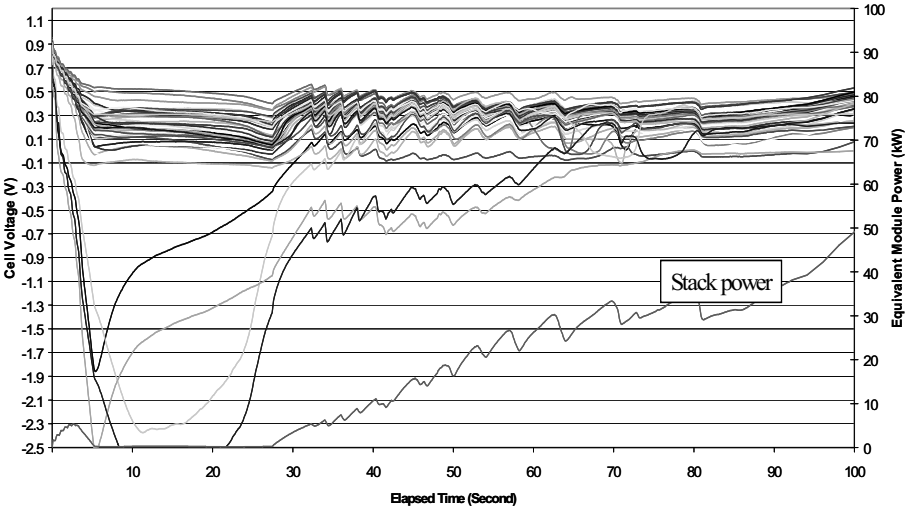

Figure 17.1. Cell voltage and equivalent module power vs. time during freeze start-up from –15 °C

Aside from the loss of power associated with one or more cells going into voltage reversal, this situation poses durability and reliability concerns as well. Undesirable electrochemical reactions may occur, which can detrimentally affect, or degrade, fuel cell components. For example, when there is an inadequate supply

of fuel (e.g., fuel starvation due to ice formation, water flooding at the anode, fuel supply problems, and the like) to a PEM fuel cell, there can be a rise in the absolute potential of the fuel cell anode, leading to electrolysis of the water present at the anode and to oxidation (e.g., corrosion) of the anode components. Such component degradation reduces the reliability and performance of the affected fuel cell and, in turn, its associated stack and array. Fuel starvation, an inadequate supply of fuel to the MEA at the anode, is the most damaging source of cell voltage reversal [17].

In this review, both cathode and anode voltage reversals, and the damage caused by voltage reversal will be presented. The development of a reversal-tolerant catalyst layer using different strategies, including enhancing water retention, using more corrosion-resistant catalyst support, and adding a water electrolysis catalyst into the anode structure will be reviewed.

17.2 Cell Voltage Reversal

17.2.1 Air Starvation

During normal operation of a PEM fuel cell on hydrogen fuel, the following electrochemical reactions take place:

$$\text{at the anode:} \quad H_2 = 2H^+ + 2e^- \tag{17.1}$$

$$\text{at the cathode:} \quad \tfrac{1}{2}O_2 + 2H^+ + 2\,e^- = H_2O \tag{17.2}$$

$$\text{overall:} \quad H_2 + \tfrac{1}{2}O_2 = H_2O \tag{17.3}$$

However, with insufficient oxidant (oxygen) present, the protons produced at the anode cross the electrolyte and combine with electrons directly at the cathode to produce hydrogen gas.

$$2H^+ + 2e^- = H_2 \quad E_{0,\,25\,^\circ C} = 0.00\ \text{V (vs. NHE)} \tag{17.4}$$

The anode reaction and the anode potential remain unchanged and the PEM fuel cell acts as a hydrogen pump. The cathode potential drops due to the lack of oxygen and the presence of hydrogen, and the cell voltage generally drops to very low levels or may even become negative. Since the oxidation of hydrogen gas and the reduction of protons are both very facile on Pt-based electrocatalysts (that is, small overpotential), the voltage across the fuel cell during this type of reversal is quite small. Hydrogen production actually begins at small positive cell voltages (for example, 0.03 V) because of the large hydrogen concentration difference present in the cell. The cell voltage observed during this type of reversal depends on several factors (including the current and cell construction) but, at current densities of about 0.5 A cm^{-2}, the fuel cell voltage may typically be more than or about –0.1 V.

An insufficient oxidant condition can arise when there is water flooding in the cathode, oxidant supply problems, and the like. Such conditions then lead to low magnitude voltage reversals with hydrogen being produced at the cathode. Significant heat may also be generated in the affected cell(s). These effects raise potential reliability concerns. However, the low potential experienced at the cathode does not typically pose a significant corrosion problem for the cathode components. Nonetheless, some degradation of the membrane may occur from the lack of water production and from the heat generated during reversal. Also, the continued production of hydrogen may result in some damage to the cathode catalyst.

17.2.2 Fuel Starvation

In a PEM fuel cell system, there can be several sources of cell voltage reversal but most damaging is fuel starvation of the cell at the anode. A different situation occurs when there is insufficient fuel present. In this case, the cathode reaction and thus the cathode potential remain unchanged. However, the anode potential rises to the potential for water electrolysis. Then, as long as water is available, electrolysis takes place at the anode. However, the potential of the anode is then generally high enough to slowly start oxidizing typical components used in the anode, for example, the carbons employed as supports for the catalyst, or the electrode substrates. Thus, some anode component oxidation typically occurs along with electrolysis. (Thermodynamically, oxidation of the carbon components actually starts to occur before electrolysis. However, it has been found that electrolysis appears to be kinetically preferred and thus proceeds at a greater rate.) The reactions in the presence of oxidizable carbon-based components are typically: at the anode in the absence of fuel:

$$H_2O = ½O_2 + 2H^+ + 2\,e \qquad {}^{-}E_{0,25\,^\circ C} = 1.23\ V \tag{17.5}$$

and

$$½C + H_2O = 2CO_2 + 2H^+ + 2e^- \qquad E_{0,25\,^\circ C} = -0.21\ V \tag{17.6}$$

More current can be sustained by the electrolysis reaction if more water is available at the anode. However, if not consumed in the electrolysis of water, current is instead used in the corrosion of the anode components. If the supply of water at the anode runs out, the anode potential rises further and the corrosion rate of the anode components increases. Thus, there is preferably an ample supply of water at the anode in order to prevent degradation of the anode components during reversal.

Studies at Ballard Power Systems [12] have shown that the electrochemical processes in this case can be monitored by following the cell voltage with time and by gas chromatographic analysis of the anode outlet gas for oxygen and CO_2 production. Figure 17.2 shows the typical response from an MEA with a carbon-supported PtRu anode. In this case, the cathode reaction and the cathode potential remain unchanged and the change in cell voltage reflects the anode potential. As

the anode is starved of fuel the anode potential increases until water electrolysis occurs (assuming water is available) (Equation 17.5). Figure 17.2 shows that at 40 mA cm^{-2}, this corresponds to a cell voltage of –0.6 V. After falling quickly to –0.6 V, the cell voltage gradually decays to –0.9 V, corresponding to an anode potential of +1.4 to +1.7 V (vs. RHE). That the resulting water electrolysis plateau in Figure 17.2 is due to Equation 17.5 was confirmed by the high current efficiency for oxygen evolution. At such a high anode potential, a small degree of carbon corrosion (Equation 17.6) accompanies water electrolysis, as shown in Figure 17.2 by the small quantity of CO_2 detected in the anode outlet gas.

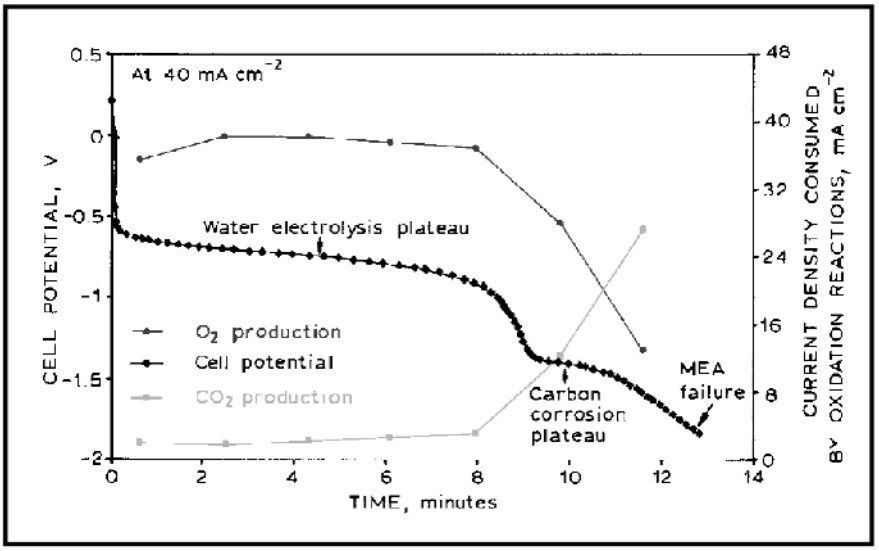

Figure 17.2. The change in the cell voltage at 40 mA cm^{-2} and the rate of oxygen and CO_2 produced at an MEA during voltage reversal due to fuel starvation. The anode is prepared from 20 wt% Pt, 10 wt% Ru/Shawinigan at a loading of 0.25 mg Pt cm^{-2}. The cathode uses Pt black at a loading of 4.0 mgPt cm^{-2}. The MEAs are based on catalyzed substrates bonded to Nafion NE-1135 membrane. Operating conditions: nitrogen (at the anode, replicating fuel starvation)/air, 200/200 kPa, 1.5/2 stoichiometry. The oxygen and CO_2 were detected in the anode outlet gas using gas chromatography [17]. (Reprinted from Ralph TR, Hogarth MP. Catalysis for low temperature fuel cells, part II: the anode challenges, Plat Met Rev 2002;46(3):117–35. With permission from Platinum Metals Review.)

If the supply of water to the anode electrocatalyst runs out or if the Pt-based anode electrocatalyst is deactivated for water electrolysis, the cell voltage moves to more negative potentials. Figure 17.2 shows a carbon corrosion plateau as the cell voltage reaches –1.4 V, corresponding to an anode potential of +2.1 V (vs. RHE). At this stage the current is sustained increasingly by carbon corrosion rather than by water electrolysis, as shown in Figure 17.2 by the increase in the rate of CO_2 production and the decrease in the rate of oxygen production in the anode chamber. Significant irreversible damage to the MEA occurs since the anode electrocatalyst carbon support, the anode gas diffusion substrate and the anode flow field plate (if

carbon-based) all corrode. After a few minutes in this condition the MEA is normally electrically shorted due to the significant amount of heat generated in the membrane.

It can be seen that the voltage of a fuel cell experiencing fuel starvation is generally much lower than that of a fuel cell receiving insufficient oxidant. During reversal from fuel starvation, the cell voltage ranges around –1 V when most of the current is carried by water electrolysis. However, when electrolysis cannot sustain the current (for example, if the supply of water runs out or is inaccessible), the cell voltage can drop substantially (to much less than –1 V) and is theoretically limited only by the voltage of the remaining cells in the series stack. Current is then carried by corrosion reactions of the anode components or through electrical shorts, including dielectric breakdown of the membrane electrolyte, which may develop as a result. Additionally, the cell may dry out, leading to very high ionic resistance and further heating. The impedance of the reversed cell may increase such that the cell is unable to carry the current provided by the other cells in the stack, thereby further reducing the output power provided by the stack.

Fuel starvation can arise when there is severe water flooding at the anode, fuel supply problems, and the like. Such conditions then lead to high-magnitude voltage reversals (i.e., the cell voltage can drop to less than –1 V) with oxygen being produced at the anode. Significant heat may again be generated in the reversed cell. These effects raise more serious reliability concerns than in an oxidant starvation condition. Very high potentials may be experienced at the anode, thereby posing a serious concern about anode corrosion and hence, reliability.

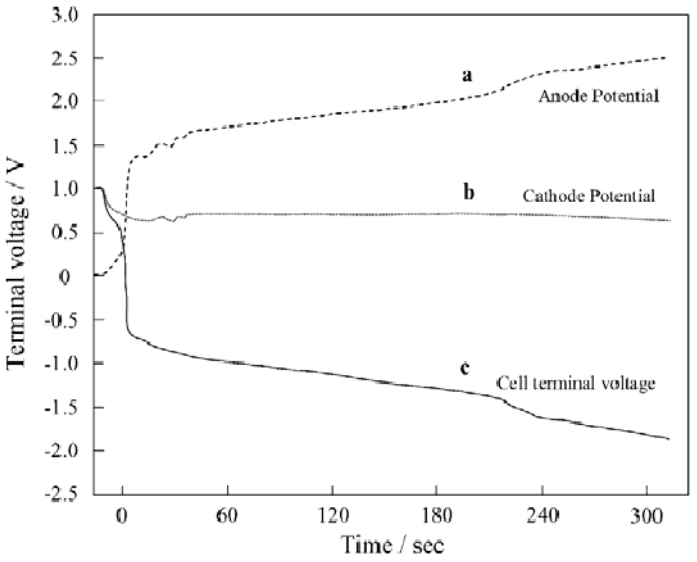

Figure 17.3. The time-dependent changes of the anode and cathode potential during the cell voltage reversal experiment [19]. (Reprinted from Journal of Power Sources, 130(1–2), Taniguchi A, Akita T, Yasuda K, Miyazaki Y, Analysis of electrocatalyst degradation in PEMFC caused by cell reversal during fuel starvation, 42–9, ©2004, with permission from Elsevier.)

The potential change of the cell terminal voltage and individual electrodes during the cell voltage reversal experiment can be measured using a reference electrode [19]. The typical time-dependent change of the cell terminal voltage during an experiment is shown in Figure 17.3. In addition, this figure shows the time-dependent change of the anode and cathode potentials versus RHE. It was observed that the cell terminal voltage rapidly dropped to a negative voltage and the MEA changed polarity due to cell voltage reversal as soon as the experiment started. After this initial rapid drop, the cell voltage showed a steady decrease with time. Cell voltage reversal occurred when the anode potential increased and became more positive than the cathode potential. As soon as the experiment began, the anode potential quickly increased to nearly 1.5 V and water electrolysis occurred because the anode was starved of fuel [17], consistent with what has been described previously [12].

17.2.3 Electrocatalyst Degradation in PEM Fuel Cells Caused by Cell Voltage Reversal During Fuel Starvation

Various circumstances can result in a fuel cell being driven into voltage reversal by other cells in the series stack. Irreversible damage to the MEAs may be caused by such cell voltage reversal incidents. The most damaging source of cell voltage reversal is reactant starvation, an inadequate supply of fuel to the MEA at the anode [17]. There are some reports about a reactant starvation problem in the phosphoric acid fuel cell (PAFC) [20–22]. In the early 1990s, Mitsuda and Murahashi studied the changes in the electrode potential in the plane of the PAFC under reactant starvation conditions, for the Moonlight Project in Japan. This work made it clear that there is a polarization distribution in the horizontal plane of PAFC electrodes, by experiment using a single cell equipped with multi-reference electrodes [21, 22]. As for the PEMFC, Sanyo Electric reported performance degradation caused by reactant starvation in a national R&D project on PEM fuel cells [23].

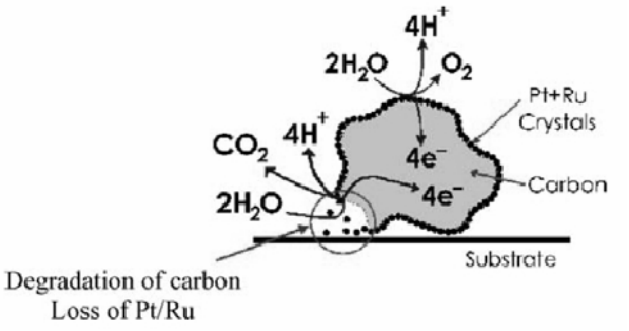

Figure 17.4. Schematic representation of degradation of carbon catalyst support during operation in the absence of fuel [18]. (Reprinted from Journal of Power Sources, 127(1–2), Knights SD, Colbow KM, St-Pierre J, Wilkinson DP, Aging mechanisms and lifetime of PEFC and DMFC, 127–34, ©2004, with permission from Elsevier.)

Most current technology development is focused on the use of platinum (or platinum and ruthenium) supported on carbon particles, in order to reduce the amount of platinum required on the anode down to 0.05–0.45 mg cm^{-2}, as described in [10]. These types of anodes are prone to degradation during fuel starvation due to the reaction in Equation 17.6, the oxidation of carbon, which is catalyzed by the presence of platinum [11]. This reaction proceeds at an appreciable rate at the electrode potentials required to electrolyze water in the presence of platinum (greater than approximately 1.4 V [24). This is shown schematically in Figure 17.4. The catalyst support is converted to CO_2, and Pt and/or Ru particles may be lost from the electrode, resulting in loss of performance.

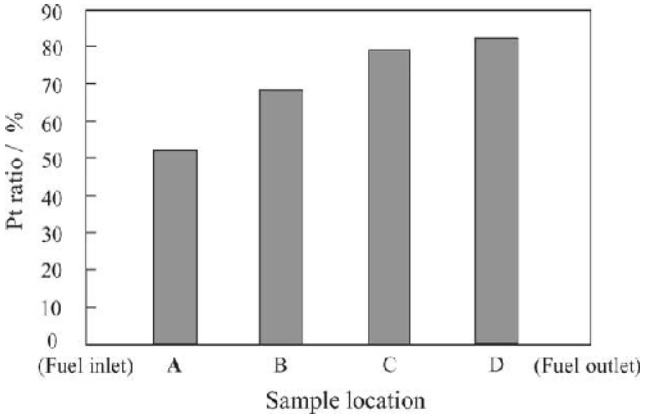

Figure 17.5. The dependence of the Pt ratio to Ru, Pt/(Ru + Pt), of the anode catalyst layer after the cell voltage reversal experiment for 2 min, determined by EDX on the sample location [19]. (Reprinted from Journal of Power Sources, 130(1–2), Taniguchi A, Akita T, Yasuda K, Miyazaki Y, Analysis of electrocatalyst degradation in PEMFC caused by cell reversal during fuel starvation, 42–9, ©2004, with permission from Elsevier.)

The damage to the electrocatalyst caused by cell voltage reversal during PEM fuel cell operation with fuel starvation was investigated by Taniguchi et al. [19]. The samples from degraded MEAs were characterized. Chemical analysis of the anode catalyst layer of MEA samples by energy dispersive X-ray analysis (EDX) was used to demonstrate ruthenium dissolution from the anode catalyst particles. The relative changes in the Pt:Ru ratio before and after the cell voltage reversal experiment provided information to assess the anode catalyst degradation. The change in the Pt:Ru ratio, Pt/(Ru + Pt), of the PEMFC anode plane under cell voltage reversal for 2 min is shown in Figure 17.5. A significant decrease in the Ru content was detected in the region located near the fuel outlet area. The platinum ratio increased from the fuel inlet region to the fuel outlet region, as shown in this figure. In the anode of PEM fuel cells operated on reformed gas for practical use, the hydrogen concentration downstream is significantly reduced compared with that upstream. This change indicates that the region where fuel starvation occurs suffers severely from degradation in the anode plane. Figure 17.6 shows the relative changes in the Pt:Ru ratio, Pt/(Ru+Pt), near the fuel outlet region before

and after the cell voltage reversal experiment, at different times. It was observed that the platinum ratio of the anode catalyst layer clearly increased after cell voltage reversal. The Pt:Ru ratio of the anode catalyst layer was also measured using X-ray photoelectron spectroscopy (XPS), as shown in this figure. Strictly speaking, the XPS measurement might not reflect the status of the interface between the catalyst layer and membrane, which is the most important electrochemical reaction zone [25], because the measurement was taken on the back surface of the catalyst layer. However, the results were similar to those measured by EDX. The values for degraded samples measured by XPS were slightly higher than those measured by EDX. Although nearly bulk information about the catalytic active particles can be obtained by XPS, since the particle size is very small, the higher Pt ratio measured by XPS possibly suggests a Pt surface-rich composition of catalyst particles.

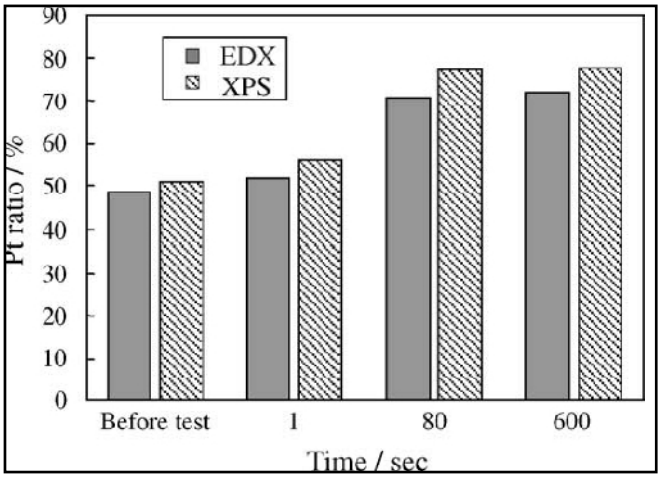

Figure 17.6. The relative changes in the Pt ratio to Ru, Pt/(Ru + Pt), near the fuel outlet region before and after the cell voltage reversal experiment at different times, determined by EDX and XPS [19]. (Reprinted from Journal of Power Sources, 130(1–2), Taniguchi A, Akita T, Yasuda K, Miyazaki Y, Analysis of electrocatalyst degradation in PEMFC caused by cell reversal during fuel starvation, 42–9, ©2004, with permission from Elsevier.)

A reduced carbon monoxide (CO) tolerance was found by CO-stripping voltammetry and measurement of deteriorated fuel cell performance. Figure 17.7 shows *I–V* curves of the cell after different experimental periods during the cell voltage reversal test. These curves were measured under the condition of enough hydrogen fuel containing 50 ppm CO being supplied. The original performance of the cell was lowered by increasing the experimental time. Notably, the performance of the cell after cell voltage reversal for 7 min showed the typical form of anode CO poisoning [26]. This kind of degradation behavior suggests deterioration of CO tolerance by the anode catalyst. The effect on the cathode was also evaluated via the *I–V* curves, under the condition of enough pure hydrogen fuel being supplied, before and after the cell voltage reversal experiment, for 10 min. A performance loss due to the cell voltage reversal was also observed, which

was attributed to the degradation of the cathode catalyst, as in the case of pure hydrogen fuel, the anode overpotential is negligible when Pt or PtRu is the anode catalyst [27].

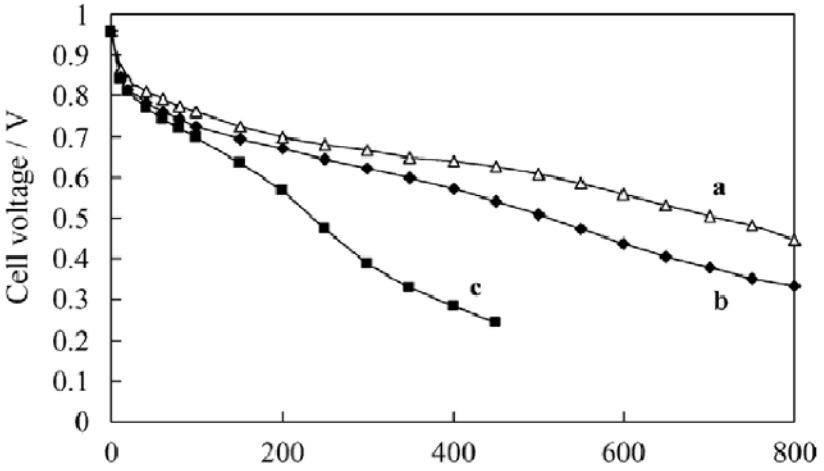

Figure 17.7. The change in current-voltage performance of a PEMFC by the cell voltage reversal experiment: (a) before experiment; (b) after experiment for 3 min; and (c) after experiment for 7 min [19]. (Reprinted from Journal of Power Sources, 130(1–2), Taniguchi A, Akita T, Yasuda K, Miyazaki Y, Analysis of electrocatalyst degradation in PEMFC caused by cell reversal during fuel starvation, 42–9, ©2004, with permission from Elsevier.)

Surface area loss of cathode platinum due to catalyst agglomeration was also detected by transmission electron microscopy (TEM) analysis and cyclic voltammetry. The behaviors of both electrodes were measured and anode degradation could be attributed to the high anode potential. Fuel starvation caused severe and permanent damage to the electrocatalysts of the PEMFC.

17.3 Development of Reversal-tolerant Catalyst Layers

The adverse effects of voltage reversal can be prevented, for instance by employing diodes [28] capable of carrying the current across each individual fuel cell or by monitoring the voltage of each individual fuel cell and shutting down an affected cell if a low voltage situation is detected. However, given the total number of individual cells in a fuel cell stack, such approaches can be quite complex and expensive to implement. Alternatively, other conditions associated with voltage reversal may be monitored instead and appropriate corrective action taken if reversal conditions are detected. For instance, a specially constructed sensor cell [29] may be employed that is more sensitive than other cells in the stack to certain conditions leading to voltage reversal (for example, fuel starvation of the stack). Thus, instead of monitoring every cell in a stack, only the sensor cell need be monitored and used to prevent widespread cell voltage reversal under such

conditions. However, other conditions leading to voltage reversal may exist that a sensor cell cannot detect (for example, a defective individual cell in the stack). Another approach is to employ exhaust gas monitors that detect voltage reversal by detecting the presence of, or abnormal amounts of, species in an exhaust gas of a fuel cell stack that originate from reactions that occur during reversal [30]. While exhaust gas monitors can detect a reversal condition occurring within cells in a stack and they may suggest the cause of the reversal, such monitors do not identify specific problem cells and they do not generally provide any warning of an impending voltage reversal.

Instead of or in combination with the preceding, a catalyst layer design approach may be preferred such that, in the event that reversal does occur, the fuel cells are either more tolerant to the reversal or are controlled in such a way that degradation of any critical component is reduced. Such an approach may be particularly preferred if the conditions leading to reversal are temporary. If the cells can be made more tolerant to voltage reversal, it may not be necessary to detect for reversal and/or shutdown the fuel cell system during a temporary reversal period. The results that demonstrated significantly improved cell voltage reversal tolerance, without compromising performance, are reported here.

17.3.1 Reversal Tolerance Cathode Catalyst Layer

Water management is one of the critical issues to be solved in the design and operation of PEM fuel cells. Water is produced at the cathode of PEMFCs. If water is not removed effectively, it accumulates at the cathode of the fuel cell, causing electrode flooding. The consequence is oxygen starvation, thus increasing the concentration overpotential of the cathode. In the worst scenarios, a proton (H^+) reduction reaction, instead of the oxygen reduction reaction (ORR), might occur at the cathode. Not only will this cause a cathode potential drop, but also the output voltage of a single cell would likely be reversed due to oxygen starvation. Particularly in the case of small fuel cells operated at room temperature, water flooding may appear [31]. If active control of water management cannot be guaranteed due to the size and power demands of the auxiliary equipment, passive possibilities of intervention are required. One alternative is to manipulate the characteristics of the used diffusion or backing layers [31, 32].

To study and resolve the voltage reversal problem, a MnO_2–Pt/C composite electrode was used by Wei et al. [33] to replace the conventional Pt/C electrode. This choice was based upon the fact that the electrochemical reduction of MnO_2 has almost the same Nernstian potential as the ORR, as shown below:

$$MnO_2 + 4H^+ + 2e^- = Mn_2^+ + 2H_2O \ (E_0 = 1.23 \text{ V}) \tag{17.7}$$

The reaction in Equation 17.7 can replace the ORR in the case of oxygen starvation. Thus, the voltage reversal effect (VRE) resulting from the proton reduction reaction (PRR) could be avoided without the use of a fan to scavenge the excess water. Two environments, N_2- and O_2-saturated H_2SO_4, were adopted to simulate two cases, i.e., O_2 starvation and O_2 richness. It was found that MnO_2–Pt/C can prevent the voltage reversal effect to a certain extent. In a N_2-saturated

1M H_2SO_4 solution, the current density of the Pt/C electrode, made of 0.6 mg Pt cm^{-2},was close to 0, while for the MnO_2–Pt/C composite electrode, made of 0.4 mg Pt cm^{-2} and 0.8 mg MnO_2 cm^{-2}, it was as high as 10 mA cm^{-2}. Though the current generated on the MnO_2–Pt/C composite electrode in the case of oxygen starvation is not as great as that in the case when it is oxygen rich, the current might be high enough for some applications, such as powering a radio, hearing-aid, and such-like miniature devices. This illustrates that the introduction of MnO_2 into the Pt/C catalyst not only can alleviate, to a certain extent, the voltage reversal problem in the case of oxygen starvation, but also can play a synergistic role with Pt/C in the catalysis of the ORR, in oxygen-rich conditions. In an O_2-saturated 1 M H_2SO_4 solution, the MnO_2 in a MnO_2–Pt/C composite electrode primarily plays a catalytic role in the ORR by enhancing the catalytic behavior of Pt for the ORR. The impedance spectra of MnO_2–Pt/C and Pt/C electrodes were carried out for the two gases in bubbled electrolyte, which further confirmed that MnO_2 in the composite electrode does substitute for oxygen as an electron-acceptor in the case of oxygen starvation. The discharged MnO_2 can then be restored to its initial state, regardless of whether it is in oxygen-rich or starved conditions.

17.3.2 Reversal Tolerance Anode Catalyst Layer

During voltage reversal, electrochemical reactions may occur that result in the degradation of certain components in the affected fuel cell. Depending on the reason for the voltage reversal, there can be a rise in the absolute potential of a fuel cell anode. This can occur, for instance, when the cause is an inadequate supply of fuel (that is, fuel starvation). During such a reversal in a solid polymer fuel cell, water present at the anode may be electrolyzed. When significant water electrolysis occurs, the fuel cell voltage typically remains above about –1 V, but this voltage depends on several variables, including the amount of water present, the amount of fuel present, the current drawn, and the temperature. It is preferable to have electrolysis occur rather than component oxidation. When water electrolysis reactions at the anode cannot keep up with the current forced through the cell, the absolute potential of the anode can rise to a point where oxidation (corrosion) of anode components takes place, typically irreversibly degrading the components. Therefore, a solid polymer fuel cell can be made more tolerant to voltage reversal by increasing the amount of water available for electrolysis during reversal, thereby channeling the current forced through the cell into the more innocuous electrolysis of water rather than the detrimental oxidation of anode components. By increasing the amount of water in the vicinity of the anode catalyst during normal operation, more water is available at the anode catalyst in the event of a reversal. Thus, modifications to the anode structure that result in more water being present at the anode catalyst during normal operation lead to improved tolerance to voltage reversal. In addition to enhancing the presence of water at the anode through modifications to the anode structure, a PEM fuel cell can be made more tolerant to voltage reversal by incorporating an additional catalyst, a water electrolysis catalyst, at the anode to promote the electrolysis of water. In these ways, more of the current being forced through the cell is consumed by the electrolysis of water than by the oxidation of the anode components.

17.3.2.1 Enhancing the Presence of Water at the Anode

In a typical PEM fuel cell, water generated at the cathode diffuses through the polymer membrane to the anode. Restricting the passage of this water through the anode structure and into the exhaust fuel stream means more water remains in the vicinity of the catalyst. This can be accomplished, for example, by making the anode catalyst layer or an anode sublayer impede the flow of water (in either vapor or liquid phase) [17, 18, 30]. For instance, adding a hydrophobic material such as polytetrafluoroethylene (PTFE) to either of these layers makes them more hydrophobic, thereby hindering the flow of water through the anode. Figure 17.8 shows the benefit of adding PTFE to the anode catalyst layer to enhance the voltage reversal tolerance. The cell voltage response over time of different four-cell stacks with different anode designs is also shown. Each stack was subjected to fuel starvation conditions through an equivalent number of cycles, then finally starved of hydrogen and allowed to go into voltage reversal until an average cell voltage of –2 V was reached. The length of time the cells operated prior to reaching –2 V is a measure of robustness to fuel starvation. Addition of PTFE into the anode catalyst layer extended the reversal time to more than 20 minutes from less than 5 minutes. The reversal tolerance was improved more than 4 times simply by the addition of PTFE into the anode catalyst layer.

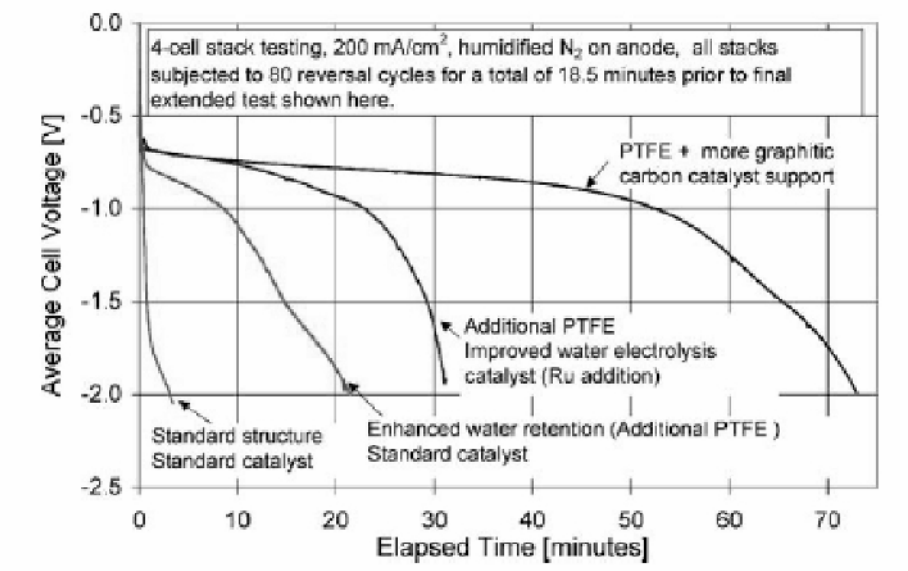

Figure 17.8. Comparison of different anode structures in severe failure testing. Each cell has an equivalent cathode (~0.7 mg cm^{-2} Pt, supported on carbon). Testing was conducted at 200 mA cm^{-2} with fully humidified nitrogen on the anode. Anode loading was ~0.3 mg cm^{-2} Pt supported on carbon (varied materials and compositions). Each curve represents the results from a 4-cell stack, each cell of identical composition. Four separate stack tests were run to generate the curves [18]. (Reprinted from Journal of Power Sources, 127(1–2), Knights SD, Colbow KM, St-Pierre J, Wilkinson DP, Aging mechanisms and lifetime of PEFC and DMFC, 127–34, ©2004, with permission from Elsevier.)

Alternatively, other additives (for example, graphite, other carbons, or titanium oxide powders) may be employed to reduce the porosity of either layer, thereby impeding the flow of water through the anode. It may be advantageous to employ a porosity-reducing additive mixture of polytetrafluoroethylene and acetylene carbon black, in which the anode catalyst layer comprises between about 12% and 32% by weight of polytetrafluoroethylene and between about 0.03 and 0.2 mg cm^{-2} of acetylene carbon black.

Another approach for increasing the amount of water in the anode catalyst layer is to boost the water content in the catalyst layer components. A conventional catalyst layer, for instance, may contain up to 30% by weight amount of fully hydrated perfluorosulfonic ionomer. Thus, an increase in water content can be accomplished by increasing the amount of the water-containing ionomer used in the catalyst layer or by employing a different ionomer with higher water content. Alternatively, more hygroscopic materials may be incorporated into the anode catalyst layer to retain more water therein.

The present approach makes fuel cells more tolerant to voltage reversal by facilitating water electrolysis at the anode during reversal, through providing sufficient water at the anode. It is thus an advantageous method *in situ*ations where electrolyzing more water is beneficial (for example, during a fuel starvation condition not caused by water flooding at the anode). Further, it is primarily advantageous for fuel cells operating directly on gaseous fuels. This is because liquid feed fuel cells typically employ an aqueous fuel mixture containing an abundance of water and thus an ample supply is generally already available to the anode during normal operation.

17.3.2.2 Using a More Corrosion-resistant Catalyst Support

As shown in Reaction 17.6, carbon corrosion is one of key causes of failure during voltage reversal. Using a more robust catalyst support (e.g., more graphitic carbon or non-carbon support materials) is beneficial for impeding or eliminating component degradation [14, 15, 18]. Figure 17.8 shows that using more graphitic carbon support increases the extended reversal time from ~20 minutes to 75 minutes. A more than three-fold improvement of voltage reversal tolerance was thus achieved.

It was also found that increasing catalyst coverage on the support to reduce the contact of carbon with reactants (e.g., using a higher weight percentage Pt on the carbon) [12, 13, 30, 34] is also an effective way to retard carbon corrosion. Figure 17.9 shows the cell voltage of 10-cell stacks with 2 different anode structures as a function of time during pulse reversal testing. The cells were subjected to current pulses (200 mA cm^{-2}) while operating on nitrogen and air. The pulse testing consisted of three sets of 30× on/off pulses. With the anode catalyst layer comprised of 40% Pt/20% Ru on more graphitic carbon support, the cell voltage was the same across all the 30× on/off reversal pulses (~0.8 V, at which voltage nearly all the current was consumed by water electrolysis – see Figures 17.2 and 17.3). In contrast, the anode structure consisting of 20% Pt/10% Ru on Vulcan carbon support reached –2 V at the last pulse. As has been pointed out (Figure 17.2), MEA failure occurs when the cell voltage reaches –2 V.

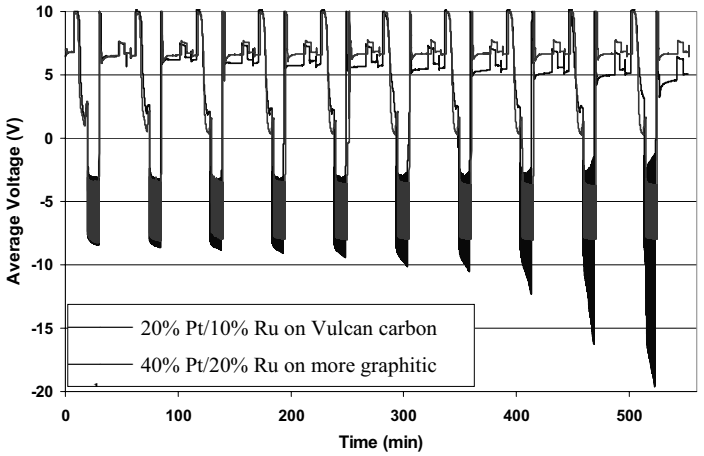

Figure 17.9. Cell voltage as a function of time during pulse reversal testing at 200 mA cm^{-2}

17.3.2.3 Addition of Water Electrolysis Catalyst

In addition to enhancing the presence of water at the anode through modifications to the anode structure, a PEM fuel cell can be made more tolerant to voltage reversal by incorporating an additional catalyst, a water electrolysis (oxygen evolution reaction, OER) catalyst, at the anode to promote the electrolysis of water [14–16, 18]. In this way, more of the current forced through the cell may be consumed by the electrolysis of water than by the oxidation of the anode components. In a reversal-tolerant fuel cell, the anode comprises a first catalyst composition for evolving protons from the fuel and a second catalyst composition for water electrolysis.

Noble metal oxides as electrocatalysts (particularly IrO_2 and RuO_2 or their mixtures – numerous investigations are concerned with oxides of rutile structure [35–40]) are well established in many industrial electrochemical processes in the form of dimensionally stable anodes (DSA), as developed by Beer [41]. RuO_2 has exhibited excellent activity in both Cl_2 and O_2 evolutions. The Tafel slope for O_2 evolution is only 0.031–0.041 V dec^{-1} in the low-potential region and 0.042–0.066 V dec^{-1} in the high-potential region [42, 43]. Unfortunately, RuO_2 and RuO_2–TiO_2, the latter widely used in the chlorine-alkali industry, are not stable for O_2 evolution in acidic environments, as their service lives are under 4 h at a current density of 0.5 A cm^{-2} in 0.25–0.5 M H_2SO_4 solutions [44, 45]. The electrochemical stability of these electrodes is significantly improved by selecting proper dispersing agents. Burke and McCarthy [46] increased the service life of the electrode by a factor of 5.3 through adding 20 molar percent of ZrO_2 to the RuO_2 layer. Iwakura and Sakamoto [45] studied the effect of adding SnO_2 to RuO_2 and found that the electrode with a molar ratio of Ru:Sn = 30:70 had a service life of about 12 h, four times longer than that of the pure RuO_2-coated electrode, under accelerated life test conditions (0.5 A cm^{-2}, 0.5 M H_2SO_4, 30 °C). Investigation of RuO_2-based DSA for oxygen evolution has continued in recent years. Oxide mixtures of interest include RuO_2–Nb_2O_5 [47], RuO_2–PbO_2 [48, 49], and RuO_2–Co_3O_4 [50]. Despite

their good activity for oxygen evolution, none of them has a service life over 20 h in accelerated life tests. Obviously, these electrocatalysts lack sufficient stability for industrial applications. The poor electrochemical stability of RuO_2-based DSA for O_2 evolution is principally due to the easy conversion of ruthenium from stable dioxide into unstable tetraoxide at a high electrical potential [51].

Recently, IrO_2-based materials have been examined for the anode or oxygen evolution electrode by Tunold et al. [52–55]. Most DSA electrodes are prepared by the thermal decomposition of metal precursors onto titanium substrates. This method is thought to be unsuitable for PEM water electrolyzers due to the difficulty of achieving good contact between the electrocatalytic layer and the membrane electrolyte. Therefore, to obtain an electrocatalytic layer on the membrane, either pre-prepared powders may be applied as an ink to the membrane [56, 57] or electrocatalytic particles can be synthesized directly on the surface or within the membrane [58, 59]. Many methods are available for the synthesis of noble metal-based oxides. The Adams fusion method [60] has been widely used to produce fine noble metal oxide powders [52–54, 61], and is based on the oxidation of metal precursors in a molten nitrate melt. Sol-gel methods have also proven useful in producing noble metal-based oxides [62–66], however, the precursor type can affect the properties of the material [66], as can the solvent removal stage [67]. Preparation of metal oxides by thermal or chemical oxidation of metallic colloids is an interesting concept as there exists a wide range of methods to synthesize such colloids [68, 69]. The polyol method is a relatively simple way to synthesize nanosized noble metal colloids such as iridium or ruthenium by the reduction of metal precursors in ethylene glycol [70, 71]. Additional steps include the separation of the metallic colloids from the ethylene glycol by centrifugation, followed by thermal oxidation in air at elevated temperatures.

Previously it has been shown that SnO_2 improves the stability of IrO_2–RuO_2 anodes in PEM water electrolyzers [61]. It has also been suggested that SnO_2 does not reduce the activity of RuO_2 as much as TiO_2 does [72]. For these reasons, the addition of SnO_2 to IrO_2 has been investigated by Tunold et al. [73]. In their previous work [74, 75], Chen et al. developed a stable ternary IrO_2–Sb_2O_5–SnO_2 electrocatalyst for O_2 evolution. In this oxide mixture, IrO_2 serves as the catalyst for O_2 evolution, SnO_2 as the dispersing agent, and Sb_2O_5 as the dopant for conductivity improvement. The service life of a Ti/IrO_2–SnO_2–Sb_2O_5 electrode containing only 10 molar percent of IrO_2 in the oxide coating is as high as 1600 h at a current density of 1 A cm^{-2} in a 3 M H_2SO_4 solution. Recently, they extended their investigation to RuO_2–Sb_2O_5–SnO_2 [76] because Ru is much cheaper and more active than Ir in oxygen evolution. In this ternary oxide coating, RuO_2 serves as the catalyst, SnO_2 as the dispersing agent, and Sb_2O_5 as the dopant. The accelerated life test showed that the Ti/RuO_2–Sb_2O_5–SnO_2 electrode containing 12.2 molar percent of RuO_2 nominally in the coating had a service life of 307 h in 3 M H_2SO_4 solution under a current density of 0.5A cm^{-2} at 25 °C, which is more than 15 times longer than other types of RuO_2-based electrodes. Instrumental analysis indicated that RuO_2–Sb_2O_5–SnO_2 was a solid solution with a compact structure, which contributed to the stable nature of the electrode. Since both SnO_2 and Sb_2O_5 are very stable chemically, the homogeneous mixing of RuO_2 with SnO_2 and Sb_2O_5 by forming a solid solution decreases the rate of RuO_2 dissolution. This

leads to a significant increase in the electrode service life. In addition, the RuO_2–SnO_2–Sb_2O_5 film has a compact structure, which further enhances the electrode stability. Their experimental results showed that RuO_2–Sb_2O_5–SnO_2 can be a very active and stable electrode for O_2 evolution. Using mixed oxides to improve the electrocatalytic properties and the stability/selectivity of the electrode has been the target of many studies [37, 38, 77–80]. De Faria et al. [81] demonstrated that partial substitution of TiO_2 by CeO_2 in a RuO_2-based electrode material improves the electrocatalytic activity for OER, but decreases the mechanical stability of the mixture. In a recent paper [82], Santana et al. reported the surface properties of the RuO_2 + TiO_2 + CeO_2 + Nb_2O_5 system and showed the instability caused by CeO_2 can be reduced introducing a small Nb_2O_5 content. They also systematically investigated the electrocatalytic properties of $[Ru_{0.3}Ti_{0.6}Ce]_{(0.1-x)}O_2[Nb_2O_5]_{(x)}$ with $(0 \leq x \leq 0.1)$ for OER (and the chlorine evolution reaction) and the stability of these oxide electrodes throughout the experiments [83]. For oxygen evolution a 30 mV Tafel slope was obtained in the presence of CeO_2, while in its absence a 40 mV coefficient was observed. The intrinsic electrocatalytic activity is mainly due to electronic factors that result from synergism between the Ru and Ce oxides. The highest global electrocatalytic activity observed for higher CeO_2 contents is attributed to electronic and geometric factors, while the true electrocatalytic activity depends on the electronic factor. The electrode stability is closely related to the composition. Comparison of the anodic voltammetric charges obtained before and after each set of experiments does not support significant electrode wear during the OER. The higher the CeO_2 content, the less stable the coating, which is probably related to the coating fragility of the porous structure formed by the CeO_2-containing oxide mixture. On the other hand, introduction of Nb_2O_5 causes a stabilization of the oxide mixture by forming a more compact layer.

Nanocrystalline oxide powders of the type $Ir_xSn_{1-x}O_2$ $(0.2 \leq x \leq 1)$ have been produced and characterized, primarily for use as oxygen evolution electrocatalysts in proton exchange membrane (PEM) water electrolyzers [73]. Two methods were used: the modified polyol method and the Adams fusion method. X-ray diffraction analysis suggests that an iridium-tin oxide solid solution with a rutile structure can be produced using the modified polyol method, with a linear relationship between lattice parameters and composition. The crystal size of the solid solution phase is below 15 nm for all compositions, indicating that the addition of tin also causes the average crystal size to increase from around 3.5 to 15 nm. The Adams fusion method resulted in at least two separate oxide phases, namely a tin-rich oxide and an iridium-rich oxide. X-ray photoelectron spectroscopy (XPS) analysis revealed no significant difference between the bulk and surface compositions, and showed that the iridium was present in at least two valent states. The electrical resistivity of the powders was compared, and an exponential increase in resistivity with tin addition was found. Overall, the resistivity measurements suggest that the limit for tin addition is around 50–60 mol% due to the high ohmic losses expected at higher tin contents in a PEM water electrolyzer.

Many studies pertaining to water electrolysis electrocatalysis in regenerative fuel cells have been published. The catalytic materials used are in general metal alloys and oxides. More recent studies have shown that Pt_1Ir_1 (numbers in subscripts indicate atomic ratios) or 50% Pt/50% IrO_2 (wt%) can be used in

regenerative fuel cells. Reasonable efficiencies and lifetimes were achieved [84–86]. Other studies have shown that Rh/Ru (1:1)-oxide and Ir/Rh (1:2)-oxide are also promising oxygen electrode catalysts in regenerative fuel cells. Chen et al. [87] showed that combinatorial discovery can be used to identify better dual-use catalysts, by superimposing activity maps to create a consensus map. Because the combinatorial method provides activity data for the entire composition space, it is more straightforwardly adapted to this task than other systematic optimization methods. Electrode arrays containing 715 unique combinations of five elements (Pt, Ru, Os, Ir, and Rh) were prepared by them via borohydride reaction of aqueous metal salts, and were screened for activity as oxygen reduction and water oxidation catalysts. Using a consensus map, catalysts that showed high activity for both reactions and good resistance to anodic corrosion were identified in the Pt–Ru-rich region of the Pt–Ru–Ir ternary. The ternary catalyst $Pt_{4.5}Ru_4Ir_{0.5}$ is significantly more active than the Pt_1Ir_1 bifunctional catalyst for both the water oxidation and oxygen reduction reactions. While the best ternary catalyst is close to Pt_1Ir_1 in composition, the latter is unstable with respect to anodic corrosion. A detailed kinetic comparison of the anodically stable catalysts $Pt_{4.5}Ru_4Ir_{0.5}$ and Pt_1Ir_1 showed that the addition of the oxophilic element Ru increases the reaction rate by stabilizing S–O bonds *(*S ≡ surface atom*)* and accelerating the oxidative deprotonation of S–OH groups. The pH dependence of the electrode kinetics was particularly useful in determining that the difference arises from stabilization of surface oxide species, which accelerates the oxidative deprotonation of surface OH groups.

To improve voltage reversal tolerance of PEM fuel cells, water electrolysis catalysts have been incorporated into anode structures by Johnson Matthey and Ballard Power Systems [12–17]. In such a reversal-tolerant fuel cell, the anode comprises a first catalyst composition for evolving protons from the fuel and a second catalyst composition for water electrolysis.

The second catalyst composition is incorporated for the purposes of electrolyzing water at the anode during voltage reversal situations. Preferred compositions thus include precious metal oxides, particularly those in the group consisting of ruthenium oxide and iridium oxide. Such oxides are characterized by the chemical formulae RuO_x and IrO_x, where x is greater than 1 and particularly about 2. Preferred compositions may also comprise mixtures and solid solutions of precious metal oxides, or mixtures and solid solutions of precious metal oxides and valve metal oxides, such as TiO_y (where y is less than or about equal to 2), for example.

Figure 17.10 shows the performance in Ballard stack hardware of three different cell-reversal-tolerant electrocatalysts prepared by Johnson Matthey. In this case the MEAs have received significant prior cell-reversal periods to drive the anodes to the limit of their tolerance. The impact that inclusion of a water electrolysis electrocatalyst has on the ability of the anode to sustain water electrolysis is evident. At the standard 40 wt% Pt, 20 wt% Ru/Shawinigan carbon black-based anode, the water electrolysis plateau is so short that it is difficult to detect. Only by using a cell reversal-tolerant electrocatalyst in the anode water electrolysis are plateaus evident in Figure 17.10. As a result, the degree of carbon corrosion is significantly reduced by the cell-reversal-tolerant electrocatalysts. The

typical PtRu anode electrocatalyst layer shows carbon corrosion after only 15 seconds of operation under the final cell-reversal conditions of Figure 17.10. This is extended to 4.5 minutes by adding RuO_2 to the electrocatalyst layer, to 24 minutes using RuO_2/TiO_2, and to 48 minutes with RuO_2/IrO_2 in the anode layer. While the carbon corrosion plateaus are not clear in Figure 17.10, the relative rate of production of CO_2 and oxygen confirmed the time scale required for significant levels of carbon corrosion. The improvement in reversal tolerance by adding a water electrolysis catalyst to the anode structure has also been demonstrated in Figure 17.8. After this extended cell-reversal testing, returning the more cell-reversal-tolerant anodes (optimized for PEMFC operation) to normal fuel cell operation indicated that there was negligible loss in the MEA power output. This contrasts with MEA failure in the absence of the water electrolysis electrocatalyst. In addition, incorporation of the water electrolysis electrocatalyst in the favored anode structures adds very little extra pgm to the MEA (< 0.1 mg cm^{-2}). Thus, this safeguard to the stack durability comes at little additional MEA cost.

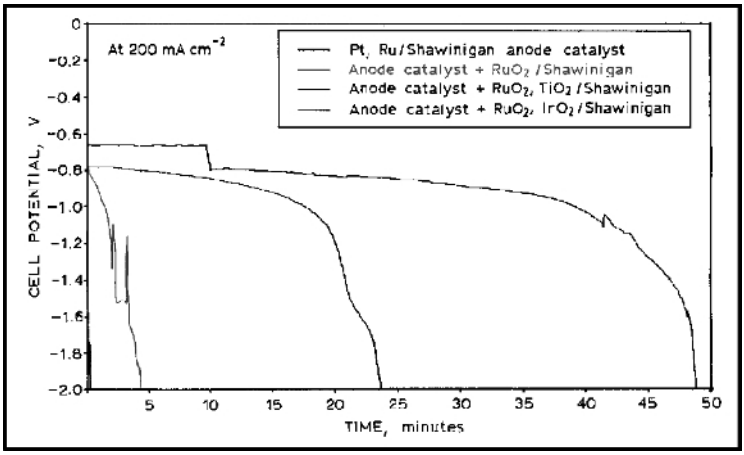

Figure 17.10. The change in cell voltage at 200 mA cm^{-2} during cell voltage reversal due to fuel starvation at a $Pt_{0.5}Ru_{0.5}$ alloy anode containing different water electrolysis electrocatalysts. The MEAs were first subjected to cell voltage reversal at 200 mA cm^{-2} for 5 minutes, then for 3 sets of 30 pulses (10 seconds on, 10 seconds off) with 15-minute recovery periods on hydrogen/air, completed by a final overnight recovery period. The anode loading is 0.1 mg Pt cm^{-2}. The water electrolysis electrocatalysts were prepared from 20 wt% RuO_2/Shawinigan, 20 wt% RuO_2, TiO_2/Shawinigan or 20 wt% RuO_2, IrO_2/Shawinigan and added at an anode loading of 0.1 mg Ru cm^{-2} [17]. (Reprinted from Ralph TR, Hogarth MP. Catalysis for low temperature fuel cells, part II: the anode challenges, Plat Met Rev 2002;46(3):117–35. With permission from Platinum Metals Review.)

Further voltage-reversal tolerance can be obtained by 1) employing a catalyst support that is more resistant to oxidative corrosion than conventional catalyst supports, 2) using certain anodes with a higher catalyst loading or coverage on a corrosion-resistant support, and 3) incorporating an additional or second catalyst

composition that promotes the electrolysis of water. A significant improvement in reversal tolerance (over 100 times greater than for a conventional anode) has been obtained by employing 2) and 3) [14–16]. Figure 17.11 shows the cell voltage during reversal testing (at 200 mA cm^{-2}) for different anode designs, where the time when the cell voltage reached –2 V was used as the criterion for reversal tolerance (see Figure 17.2). It can be seen from Figure 17.11 that improvement in reversal tolerance appeared with the incorporation of a second catalyst composition for the electrolysis of water (RuO_2 was used here) to a conventional (e.g., Vulcan) carbon-supported Pt/Ru, used as a baseline design here (15 and 28 minutes, respectively, were spent when the cell voltage reached –2 V). When using a more corrosion-resistant catalyst support (e.g., Shawinigan) for Pt/Ru plus a second catalyst composition for the electrolysis of water ($RuIrO_2$ was used here), further improvement in reversal tolerance was demonstrated. With the increase of metal content on the Shawinigan support (40% Pt/20% Ru over 20% Pt/10% Ru, supported on Shawinigan, with the same platinum loading of the anode, even with no additional catalyst to promote water electrolysis), the improvement over the previous anode design was evident (it took 167 minutes to reach –2 V). The most significant improvement in reversal tolerance among all of the other anode designs was manifested when incorporating both a more corrosion-resistant catalyst (40% Pt/20% Ru supported on Shawinigan) and a second catalyst composition for the electrolysis of water (e.g., $RuIrO_2$). This design was operated under extended reversal conditions for 2515 minutes before the cell voltage reached –2 V (167 times longer than the baseline design). Furthermore, this design demonstrated lower performance loss (less than 30 mV on air/H_2) than the other designs even though it was operated in reversal for a much longer time.

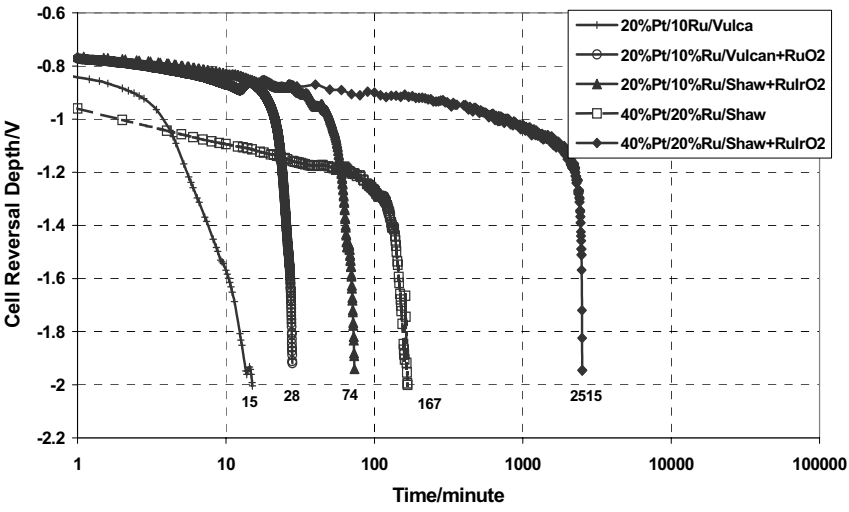

Figure 17.11. The change in cell voltage at 200 mA cm^{-2} during cell voltage reversal due to fuel starvation at different anode catalyst layer structures. The MEAs were first subjected to cell voltage reversal at 200 mA cm^{-2} for 5 minutes, then for 3 sets of 30 pulses (10 seconds on, 10 seconds off), with 15-minute recovery periods on hydrogen/air and a final overnight recovery period.

17.4 Conclusions

An overview of cell voltage reversal due to reactant starvation has been presented. A major durability issue arises at the anode if the MEA is starved of fuel. Cell voltage reversal tolerance can be improved by 1) enhancing the water retention in the anode structure, 2) employing a catalyst support that is more resistant to oxidative corrosion than conventional catalyst supports, 3) using certain anodes with a higher catalyst loading or coverage on a corrosion-resistant support, and 4) incorporating a second or additional catalyst composition that promotes the electrolysis of water. A significant improvement in reversal tolerance (over 100 times greater than that of a conventional anode) has been obtained by a combination of those strategies.

It has been demonstrated that increased durability/reliability are possible without sacrificing performance, through the careful selection of appropriate materials.

The use of reversal-tolerant cells has significant benefits for PEM fuel cell technology development:

- significantly increases the reliability
- much longer lifetime due to increased durability
- excellent operational flexibility under a wide range of operating conditions.

Acknowledgements

The author would like to acknowledge support from the R&D and Product Development Departments of Ballard Power Systems.

References

1. US Department of Energy [homepage on the Internet]. Washington, DC. c2007 [updated 2007 Oct]. DOE Multi-year research, development and demonstration plan: planned program activities for 2005–2015. Available from: http://www1.eere.energy.gov/hydrogenandfuelcells/mypp/pdfs/fuel_cells.pdf
2. Cleghorn SJC, Mayfield DK, Moore DA, Moore JC, Rusch G, Sherman TW, et al. A polymer electrolyte fuel cell life test: 3 years of continuous operation. J Power Sources 2006;158:446–54.
3. Borup RL, Davey JR, Garzon FH, Wood DL, Inbody MA. PEM fuel cell electrocatalyst durability measurements. J Power Sources 2006;163:76–81.
4. Li J, He P, K Wang, Davis M, Ye S. Characterization of catalyst layer structural changes in PEMFC as a function of durability testing. ECS Transactions 2006;3.1:743–51.
5. Ye S, Hall M, Cao H, He P. Degradation resistant cathodes in polymer electrolyte membrane fuel cells. ECS Transactions 2006;3.1:657–66.
6. Borup R, Meyers J, Pivovar B, Kim YS, Mukundan R, Nancy G. et al. Scientific aspects of polymer electrolyte fuel cell durability and degradation. Chem Rev 2007;107:3904–51.

7. Hao T, Zhigang Q, Manikandan R, Elter JF. PEM fuel cell cathode carbon corrosion due to the formation of air/fuel boundary at the anode. J Power Sources 2006;158:1306–12.
8. Yu X, Ye S. Recent advances in activity and durability enhancement of Pt/C catalytic cathode in PEMFC Part I. Physico-chemical and electronic interaction between Pt and carbon support, and activity enhancement of Pt/C catalyst. J Power Sources 2007;172:133–44.
9. Yu X, Ye S. Recent advances in activity and durability enhancement of Pt/C catalytic cathode in PEMFC Part II: Degradation mechanism and durability enhancement of carbon supported platinum catalyst. J Power Sources 2007;172:145–54.
10. Costamagna P, Srinivasan S. Quantum jumps in the PEMFC science and technology from the 1960s to the year 2000: part i. fundamental scientific aspects. J Power Sources 2001;102:242–52.
11. Passalacqua E, Vivaldi M, Giordano N, Anotonucci PL, Kinoshita K. In: Proceedings of the 27th intersociety energy conversion engineering conference. 1992;929294:3.425–31.
12. Knights SD, Wilkinson DP, Campbell SA, Taylor JL, Gascoyne JM, Ralph TR. PCT WO 01/15247 A2, 1 March 2001.
13. Taylor JL, Wilkinson DP, Wainwright DS, Ralph TR, Knights SD. PCT WO 01/15249 A2, 1 March 2001.
14. Ye S, Beattie P, Campbell SA, Wilkinson DP. Anode catalyst compositions for a voltage reversal tolerant fuel cell. US Patent Appl 2004/0013935.
15. Ye S, Beattie P, Bai K. 2005 Fuel Cell Seminar. November 14–18, 2005. Palm Springs, CA, USA.
16. Ye S, Stability of anode catalysts and their effect on PEMFC performance degradation. Presentation to Gordon Research Conference, July 22–27, 2007. Bryant University, Rhode Island, USA.
17. Ralph TR, Hogarth MP. Catalysis for low-temperature fuel cells, Part II: the anode challenges. Platinum Metals Rev 2002;46:117–35.
18. Knights SD, Colbow KM, St-Pierre J, Wilkinson DP. Aging mechanisms and lifetime of PEFC and DMFC. J Power Sources 2002;127:127–34.
19. Taniguchi A, Akita T, Yasuda K, Miyazaki Y. Analysis of electrocatalyst degradation in PEMFC caused by cell reversal during fuel starvation. J Power Sources 2004;130:42–9.
20. Tsutsumi Y, Sone I, Nanba Y. In: Abstract of the 1986 fuel cell seminar. 1986 Oct 26–29; Tucson, AZ; 110.
21. Mitsuda K, Murahashi T. Air and fuel starvation of phosphoric acid fuel cells: a study using a single cell with multi-reference electrodes. J Appl Electrochem 1991;21:524–30.
22. Mitsuda K, Murahashi T. Polarization study of a fuel cell with four reference electrodes. J Electrochem Soc 1990;137:3079–85.
23. Sakamoto S, Karakane M, Maeda H, Miyake Y, Susai T, Isono T. In: Abstract of the 2000 fuel cell seminar. 2000 Oct 30–Nov 2; Portland, OR;141.
24. Billings RE. The hydrogen world view. Independence, MO: American Academy of Science, 1991.
25. Bevers D, Wohr M, Yasuda K, Oguro K. Simulation of a polymer electrolyte fuel cell electrode. J Appl Electrochem 1997;27:1254–64.
26. Lemons RA. Fuel cells for transportation. J Power Sources 1990;29:251–64.
27. Bernadi D, Verbrugge M. A mathematical model of the solid-polymer-electrolyte fuel cell. J Electrochem Soc 1992;139:2477–91.

28. Knights SD, De Vaal JW, Lauritzen MV, Wilkinson DP. Electrochemical fuel cell stack having a plurality of integrated voltage reversal protection diodes. US Patent 7235315. 2007.
29. Barton RH. Cell voltage monitor for a fuel cell stack. US Patent 6724194. 2004.
30. Knights SD, Taylor JL, Wilkinson DP, Wainwright DS. Fuel cell anode structures for voltage reversal tolerance. US Patent 6517962. 2003.
31. Tüber K, Pócza D, Hebling C. Visualization of water buildup in the cathode of a transparent pem fuel cell. J Power Sources 2003;124:403–14.
32. Park GG, Sohn YJ, Yang TH, Yoon YG, Lee WY, Kim CS. Effect of PTFE contents in the gas diffusion media on the performance of PEMFC. J Power Sources 2004;131:182–7.
33. Wei ZD, Ji MB, Hong Y, Sun CS, Chan SH, Shen PK. MnO_2–Pt/C composite electrodes for preventing voltage reversal effects with polymer electrolyte membrane fuel cells.J Power Sources 2006;160:246–51.
34. Knights SD, Taylor JL, Wilkinson DP, Campbell SA. PCT WO 01/15254 A2, 1 March 2001.
35. Tomcsányi L, De Battisti A, Hirschberg G, Varga K, Liszi J. The study of the electrooxidation of chloride at RuO_2/TiO_2 electrode using CV and radiotracer techniques and evaluating by electrochemical kinetic simulation methods. Electrochim Acta 1999;44:2463–72.
36. Consonni V, Trasatti S, Pollak F, O'Grady WE. Mechanism of chlorine evolution on oxide anodes study of pH effects. J Electroanal Chem 1987;228:393–406.
37. De Faria LA, Boodts JFC, Trasatti S. Electrocatalytic properties of Ru + Ti + Ce mixed oxide electrodes for the Cl_2 evolution reaction. Electrochim Acta 1997;42:3525–50.
38. Arikado T, Iwakura C, Tamura H. Some oxide catalysts for the anodic evolution of chlorine: reaction mechanism and catalytic activity. Electrochim Acta 1978;23:9–15.
39. Alves VA, Da Silva LA, Boodts JFC, Trasatti S. Kinetics and mechanism of oxygen evolution on IrO_2-based electrodes containing Ti and Ce acidic solutions. Electrochim Acta 1994;39:1585–9.
40. Mráz R, Srb V, Tich´y S. Experimental activation energies for evolution of oxygen and chlorine on oxide electrodes. Electrochim Acta 1973;18:551–4.
41. Beer H. British Patent 1,147,442. 1969.
42. Yeo RS, Orehotsky J, Visscher W, Srinivasan S. Ruthenium-based mixed oxides as electrocatalysts for oxygen evolution in acid electrolytes. J Electrochem Soc 1981;9:1900–4.
43. Melsheimer J, Ziegler D. The oxygen electrode reaction in acid solution on RuO_2 electrode prepared by the thermal decomposition method. Thin Solid Films 1988;163:301–8.
44. Loucka T. The reason for the loss of activity of titanium anodes coated with a layer of RuO_2 and TiO_2. J Appl Electrochem 1977;7:211–4.
45. Iwakura C, Sakamoto K. Effect of active layer composition on the service life of (SnO_2 and RuO_2)-coated Ti electrodes in sulfuric acid solution. J Electrochem Soc 1985;132:2420–3.
46. Burke LD, McCarthy M. Oxygen gas evolution at, and deterioration of, RuO_2/ZrO_2-coated titanium anodes at elevated temperature in strong base. Eletrochim Acta 1984;29:211–6.
47. Terezo AJ, Pereira EC. Preparation and characterization of Ti/RuO_2–Nb_2O_5 electrodes obtained by polymeric precursor method. Electrochim Acta 1999;44:4507–13.
48. Musiani M, Furlanetto F, Bertoncello R. Electrodeposited PbO_2+RuO_2: a composite anode for oxygen evolution from sulphuric acid solution. J Electroanal Chem 1999;465:160–7.

49. Bertoncello R, Cattarin S, Frateur I, Musiani M. Preparation of anodes for oxygen evolution by electrodeposition of composite oxides of Pb and Ru on Ti. J Electroanal Chem 2000;492:145–9.
50. Da Silva LM, De Faria LA, Boodts JFC. Electrochemical impedance spectroscopic (EIS) investigation of the deactivation mechanism, surface and electrocatalytic properties of Ti/RuO_2(x)+Co_3O_4(1−x) electrodes. J Electroanal Chem 2002;532:141–50.
51. Hine F, Yasuda M, Noda T, Yoshida T, Okuda J. Electrochemical Behavior of the oxide-coated metal anodes. J Electrochem Soc 1979;126:1439–45.
52. Rasten E, Hagen G, Tunold R. Proc. energy and electro chemical processes for a cleaner environment. Pennington, NJ: The Electrochemical Society, 1991;151.
53. Rasten E, Hagen G, Tunold R. Electrocatalysis in water electrolysis with solid polymer electrolyte. Electrochim Acta 2003;48:3945–52.
54. Marshall A, Børresen B, Hagen G, Tsypkin M, Tunold R. First European hydrogen energy conference. 2003 Sep 2–5; Grenoble, France; CO1/71.
55. Marshall A, Børresen B, Hagen G, Tsypkin M, Tunold R. Nanocrystalline $Ir_xSn_{(1-x)}O_2$ electrocatalysts for oxygen evolution in water electrolysis with polymer electrolyte – effect of heat treatment. J New Mat Electrochem Syst 2004;7:197–204.
56. Gottesfeld S, Zawodzinski T. Polymer electrolyte fuel cells. In: Advances in electrochemical science and engineering. Alkire RC, Gerischer H, Kolb DM, Tobias CW, editors. Vol. 5. New York: Wiley, 1997;195–301.
57. Wilson M, Gottesfeld S. Thin-film catalyst layers for polymer electrolyte fuel cell electrodes. J Appl Electrochem 1992;22:1–7.
58. Millet P, Pineri M, Durand R. New solid polymer electrolyte composites for water electrolysis. J Appl Electrochem 1989;19:162–6.
59. Takenaka H, Torikai E, Kawami Y, Wakabayashi N. Solid polymer electrolyte water electrolysis. Int J Hydrogen Energy 1982;7:397–403.
60. Adams R, Shriner R. Platinum oxide as a catalyst in the reduction of organic compounds. III. Preparation and properties of the oxide of platinum obtained by the fusion of chloroplatinic acid with sodium nitrate. J Am Chem Soc 1923;45:2171–9.
61. Hutchings R, Müller L, Stucki S. A structural investigation of stabilized oxygen evolution catalysts.J Mater Sci 1984;19:3987–94.
62. Murakami Y, Ohkawauchi H, Ito M, Yahikozawa K, Takasu Y. Preparations of ultrafine IrO_2-SnO_2 binary oxide particles by a sol-gel process. Electrochim Acta 1994;39:2551–4.
63. Murakami Y, Tsuchiya S, Yahikozawa K, Takasu Y. Preparation of ultrafine IrO_2-Ta_2O_5 binary oxide particles by a sol-gel process. Electrochim Acta 1994;39:651–4.
64. Ito M, Murakami Y, Kaji H, Ohawauchi H, Yahikozawa K, Takasu Y. Preparation of ultrafine RuO_2-SnO_2 binary oxide particles by a sol-gel process. J Electrochem Soc 1994;141:1243–5.
65. Kameyama K, Shohji S, Onoue S, Nishimura K, Yahikozawa K, Takasu Y. Preparation of ultrafine RuO_2-TiO_2 binary oxide particles by a sol-gel process. J Electrochem Soc 1993;140:1034–7.
66. Lassali T, Boodts J, Bulhoes L. Effect of Sn-precursor on the morphology and composition of $Ir_{0.3}Sn_{0.7}O_2$ oxide films prepared by sol–gel process. J Non-Cryst Solids 2000;273:129–34.
67. Boiadjieva T, Cappelletti G, Ardizzone S, Rondinini S, Vertova A. Nanocrystalline titanium oxide by sol–gel method. The role of the solvent removal step. Phys Chem Chem Phys 2003;5:1689–94.
68. Bönnemann H, Richards R. Nanoscopic Metal Particles – Synthetic Methods and Potential Applications**.** Euro J Inorg Chem 2001;2001:2455–80.

69. Toshima N, Yonezawa T. Bimetallic nanoparticles—novel materials for chemical and physical applications. New J Chem 1998;22:1179–201.
70. Bonet F, Delmas V, Grugeon S, Herrera-Urbina R, Silvert P, Tekaia-Elhsissen K. Synthesis of monodisperse Au, Pt, Pd, Ru and Ir nanoparticles in ethylene glycol. Nanostruct Mater 1999;11:1277–84.
71. Kurihara L, Chow G, Schoen P. Nanocrystalline metallic powders and films produced by the polyol method. Nanostruct Mater 1995;5:607–13.
72. Trasatti S. Physical electrochemistry of ceramic oxides. Electrochim Acta 1991;36:225–41.
73. Marshall A, Børresen B, Hagen G, Tsypkin M, Tunold R. Preparation and characterisation of nanocrystalline $Ir_xSn_{1-x}O_2$ electrocatalytic powders. Mater Chem Phys 2005;94:226–32
74. Chen XM, Chen GH, Yue PL. Stable Ti/IrO_x-Sb_2O_5-SnO_2 Anode for O_2 Evolution with Low Ir Content. J Phys Chem B 2001;105:4623–8.
75. Chen GH, Chen XM, Yue PL. Electrochemical Behavior of Novel Ti/IrO_x-Sb_2O_5-SnO_2 Anodes. J Phys Chem B 2002;106:4364–9.
76. Chen X, Chen G. Stable Ti/RuO_2–Sb_2O_5–SnO_2 electrodes for O_2 evolution. Electrochim Acta 2005;50:4155–9.
77. De Faria LA, Boodts JFC, Trasatti S. Physico-chemical and electrochemical characterization of Ru-based ternary oxides containing Ti and Ce. Electrochim Acta 1992;37:2511–8.
78. Da Silva LM, Boodts JFC, De Faria LA. Oxygen evolution at RuO_2(x)+Co_3O_4(1−x) electrodes from acid solution. Electrochim Acta 2001;46:1369–75.
79. De Pauli CP, Trasatti S. Composite materials for electrocatalysis of O_2 evolution: IrO_2+SnO_2 in acid solution. J Electroanal Chem 2002;538:145–51.
80. Da Silva LM, Boodts JFC, De Faria LA. Chlorine evolution reaction at Ti/(RuO_2 +Co_3O_4) electrodes. J Braz Chem Soc 2003;14:388–95.
81. De Faria LA, Boodts JFC, Trasatti S. Electrocatalytic properties of ternary oxide mixtures of composition $Ru_{0.3}Ti_{(0.7-x)}Ce_xO_2$: oxygen evolution from acidic solution. J Appl Electrochem 1996;26:1195–9.
82. Santana MHP, Da Silva LM, De Faria LA. Investigation of surface properties of Ru-based oxide electrodes containing Ti, Ce and Nb. Electrochim Acta 2003;48:1885–91.
83. Santana MHP, De Faria LA. Oxygen and chlorine evolution on RuO_2+ TiO_2 + CeO_2 + Nb_2O_5 mixed oxide electrodes. Electrochim Acta 2006;51:3578–85.
84. Dhar HP. A unitized approach to regenerative solid polymer electrolyte fuel cells. J Appl Electrochem 1992;23:32–7.
85. Shao Z, Yi B, Han M. Bifunctional electrodes with a thin catalyst layer for ‘unitized' proton exchange membrane regenerative fuel cell. J Power Sources 1999;79:82–5.
86. Swette LL, Laconti AB, McCatty SA. Proton-exchange membrane regenerative fuel cells. J Power Sources 1994;47:343–51.
87. Chen G, Delafuente DA, Sarangapani S, Mallouk TE. Combinatorial discovery of bifunctional oxygen reduction – water oxidation electrocatalysts for regenerative fuel cells. Catalysis Today 2001;67:341–55.